A study of Silicon Photomultiplier's Pulse Structure

Paola Avella[1*], Antonella De Santo[2], Annika Lohstroh[1], Muhammad T. Sajjad[1,3], Paul J. Sellin[1]

[1]Department of Physics, University of Surrey, Guildford, UK, Member of the South East Physics Network (SEPnet)

[2]Department of Physics and Astronomy, University of Sussex, Falmer, UK, Member of the South East Physics Network (SEPnet)

[3]Advanced Technology Institute, University of Surrey, Guildford, UK

* **Correspondence author:** p.avella@surrey.ac.uk

– Introduction –

Radiation detection with scintillators and photomultiplier tubes (PMTs) has been largely used so far in applications ranging from High Energy Physics to Medical Physics as well as homeland security. However, some problems due to the magnetic field sensitivity of PMTs and the high cost of the devices related to quite difficult production processes, have encouraged the exploration of new devices with similar characteristics. Silicon Photomultipliers (SiPMs) are the solid-state equivalent of PMTs, with the advantages of single-photon counting capability, very high time resolution (about 100 ps), comparable gain (10^6) , improved photo detection efficiency for higher wavelengths, magnetic field insensitivity, small size and ultimately very low cost. They are made of a matrix of pixels that are Geiger-Mode Avalanche Photodiodes (GM-APD) connected in parallel to the same Silicon substrate. These APDs work like binary devices, detecting solely the presence of photons, but the SiPM as a whole acts as an analog device. However, the device structure, the packaging of pixels and the solid state nature of SiPMs involve new problems like non-linearity, dark noise, after-pulsing and crosstalk.

1. Static characterization

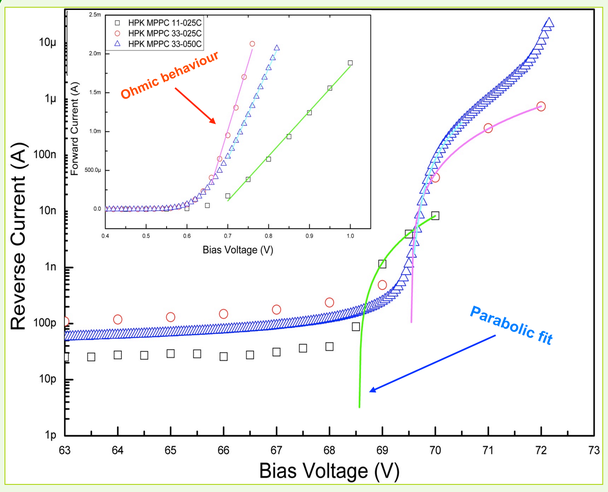

Fig. 1.1: MPPC IV forward and reverse characteristics

The measurement of the dark current that flows in the SiPM as a function of the bias voltage gives information on the topology of the device and on fundamental operational parameters like the ***quenching resistance*** and the ***breakdown voltage***. From the performed measurement the Hamamatsu MPPCs appeared to be n-type devices.

The breakdown voltages were calculated from a parabolic fit to the reverse characteristics, while a linear fit to the Ohmic part of the forward characteristics was used to obtain the total resistance of the detector. Considering that the SiPM is a matrix of pixels in parallel, the value of the resistance in series with each pixel was calculated. These plots are shown in **Fig. 1.1**, while the values aforementioned are reported in **Table 2** below.

Using an Agilent LCR meter and dedicated LabVIEW software, the values of the ***total capacitance*** and ***conductance*** for each sensor were measured at 1 V AC voltage and at 1 MHz frequency as shown in **Fig. 1.2**.

The thickness of the depletion region of the studied sensors was calculated using equation **Eq. 1.1** and the values are obtained reported in **Tab. 1**.

$$d = \varepsilon_{Si}\varepsilon_0\varepsilon_g \frac{A}{C_{meas}} \qquad \textbf{(Eq. 1.1)}$$

Device	Active Area (mm²)	Fill Factor (%)	d (μm)
HPK MPPC 11-25C	1.0 ± 0.2	30.8	1.0 ± 0.2
HPK MPPC 33-25C	9.0 ± 0.6	30.8	1.05 ± 0.07
HPK MPPC 33-50C	9.0 ± 0.6	61.5	1.88 ± 0.13

Table 1: Thickness of the depletion region

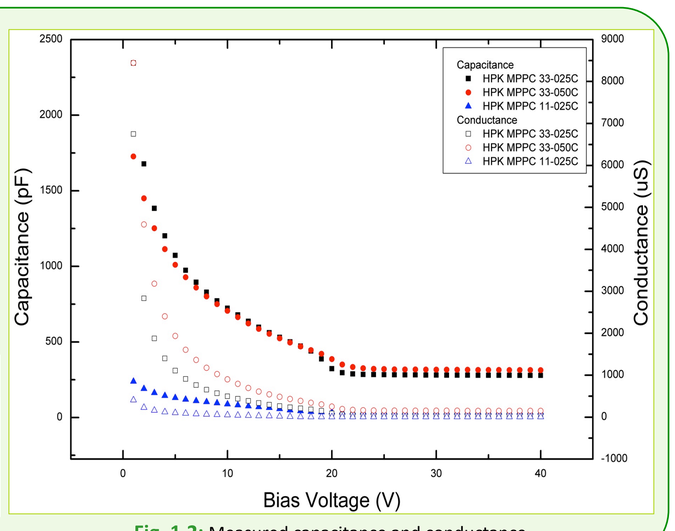

Fig. 1.2: Measured capacitance and conductance

2. Measurement of the SiPM parameters

The ***charge*** released by dark pulses was measured integrating pulses preamplified using the current amplifier Ortec VT 210. For normalization purposes an Hamamatsu Si PIN diode S1223 was used. Pulses corresponding to the interaction of α-particles from an ^{241}Am source in the Si bulk of the PIN diode and preamplified by the same preamp were acquired and integrated. The attenuation coefficient of α-particles in air (8.59 x 10^{-2} MeV/mm) was considered in the statistical error propagation, to take into account the instrumental uncertainty on the distance between the source and the detector. Equation **Eq. 2.1** describes the normalization used, were x_c is the centroid of the histograms of the integrated pulses.

$$Q_{SiPM} = Q_{PIN} \cdot \frac{x_c^{SiPM}}{x_c^{PIN}}$$

(Eq. 2.1)

Using the values measured from the static characterization and from the calculation of the ***total admittance*** of the circuit in **Fig. 2.1**, the MPPC parameters were calculated and the values shown in **Tab. 2** were obtained solving **Eq. 2.1** using a Matlab code.

$$C_d = \sqrt{G_{meas} \cdot \frac{1+\omega^2 R_q^2 C_{pixel}^2}{N_{pixel}\omega^2 R_q^2}}$$

$$C_q = C_{pixel} - C_d$$

$$C_g = C_{meas} - N_{pixel}C_d + \frac{\omega^2 N_{pixel} R_q^2 C_d^2 C_{pixel}}{1+\omega^2 R_q^2 C_{pixel}^2}$$

(Eq. 2.1)

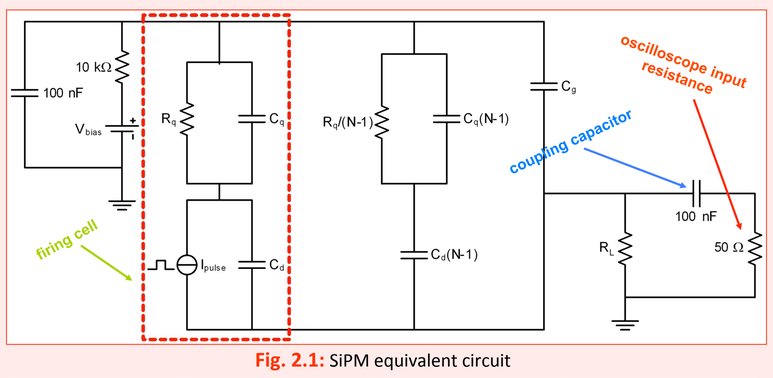

Fig. 2.1: SiPM equivalent circuit

Parameters	HPK 11-25C	HPK 33-25C	HPK 33-50C
V_{br} (V)	68.31 ± 0.06	69.25 ± 0.08	69.567 ± 0.004
R_q (kΩ)	275 ± 10	835 ± 43	371 ± 7
G_{meas} (μS)	3.064 ± 0.008	46.84 ± 0.08	139.9 ± 0.4
C_{meas} (pF)	32.82 ± 0.04	272.0 ± 0.3	304.1 ± 0.6
C_q (fF)	4.5 ± 0.9	5.6 ± 0.8	2.1 ± 1.1
C_d (fF)	13.3 ± 0.2	10.0 ± 0.2	51.9 ± 0.5
C_g (pF)	11.6 ± 0.4	129 ± 5	120 ± 10
C_{pixel} (fF)	18.0 ± 0.9	16.7 ± 0.6	54 ± 1
N_{pixel}	1600	14400	3600

Table 2: Hamamatsu MPPC measured parameters

The parameters obtained were used as input values in a PSpice simulation of the circuit in **Fig. 2.1,** simulating the interaction of only one photon in one pixel with a current pulse with a rise time of 5 ps, pulse duration of 1 ps and decay time of 90 ps. **Fig 2.3** shows the plot of the three MPPCs analysed.

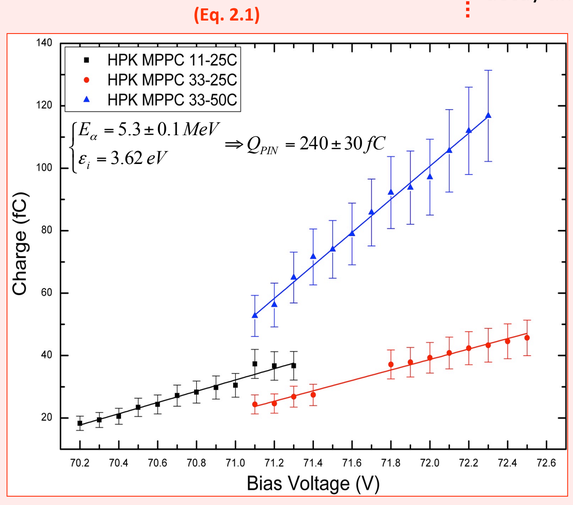

Fig. 2.2: Plots of the pulse integral versus the bias voltage

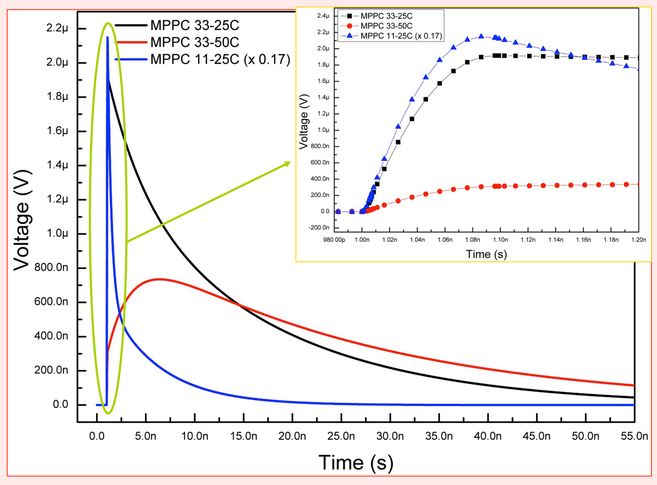

Fig. 2.3: PSpice simulation of MPPC pulses using the measured values

3. The effects of the readout electronics

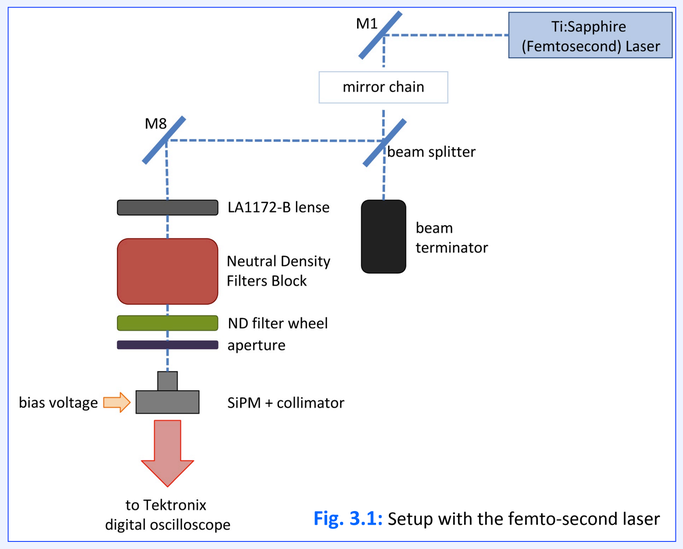

Fig. 3.1: Setup with the femto-second laser

With the parameters previously measured, a PSpice simulation of single photon pulses using different values of the ***load resistor*** was made. Increasing values of the rise time for increasing values of R_L were found.

The Hamamatsu MPPC 11-25C was chosen for the tests with different readout electronics and different laser light intensities. The plots below represent the results obtained using the setup drawn in **Fig. 3.1**.

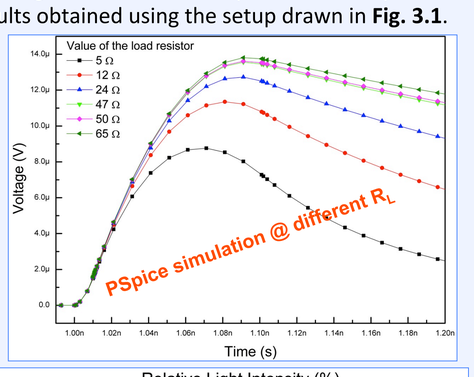

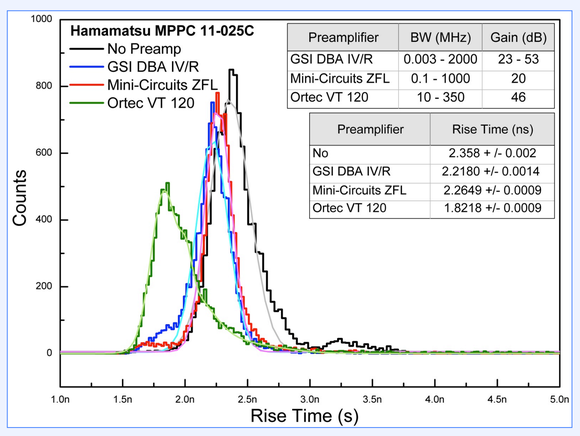

Preamplifier	BW (MHz)	Gain (dB)
GSI DBA IV/R	0.003 - 2000	23 - 53
Mini-Circuits ZFL	0.1 - 1000	20
Ortec VT 120	10 - 350	46

Preamplifier	Rise Time (ns)
No	2.358 + /- 0.002
GSI DBA IV/R	2.2180 +/- 0.0014
Mini-Circuits ZFL	2.2649 +/- 0.0009
Ortec VT 120	1.8218 +/- 0.0009

Fig. 3.2: Histograms of rise-time using different current preamplifiers at fixed light intensity

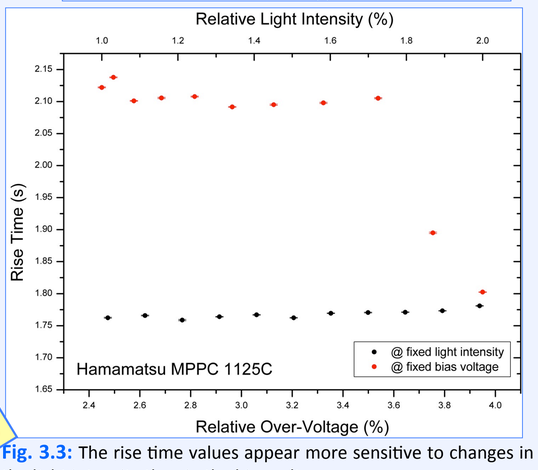

Fig. 3.3: The rise time values appear more sensitive to changes in the light intensity than in the bias voltage

NO preamp

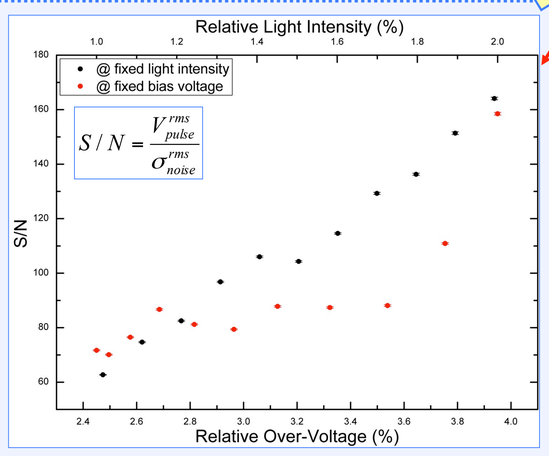

Fig. 3.4: The S/N improves as the relative parameters increase

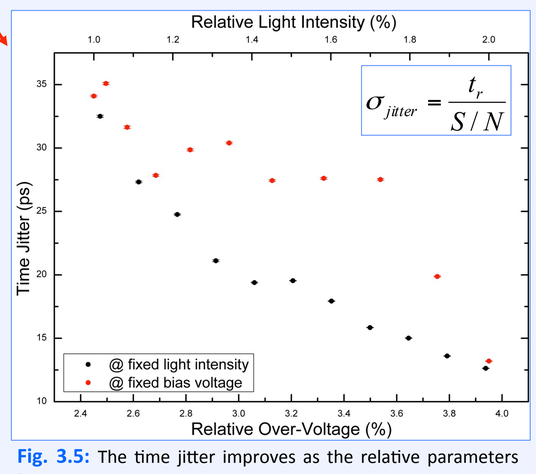

Fig. 3.5: The time jitter improves as the relative parameters increase

4. Conclusions and future developments

The parameters of selected Hamamatsu MPPCs were measured. A good agreement with the expected values was found in the case of the device terminal capacitance. The values of the quenching and diode (and total pixel) capacitance are consistent for devices with the same pixel size. The values of the parasitic capacitance associated to the metal grid that connects the pixels in parallel are consistent for MPPCs with the same active area. From a PSpice simulation the pulse rise time associated with devices with a smaller pixel size was found to be shorter, suggesting the choice of these sensors for the use in timing applications.

In the second part of the work, the effect of the readout electronics on the timing performances of the devices was studied. The results show an improvement of quantities like rise time, S/N and time jitter with the increase of the number of photons striking the device as well as with the increase of the bias voltage when the MPPC was not coupled to any preamplifier. The histogram of the rise time for different current preamplifiers shows that the best amplifier for timing applications should present mainly good noise performances when coupled to the SiPM.

The work described so far has been focused on the timing performances study of a selection of SiPMs for application in ToF-PET. Next developments will be the upgrade of the readout electronics to a faster preamplifier with higher bandwidth, gain and better S/N and a detailed study of the properties of various inorganic scintillating crystals with a very fast response, high density, atomic number and high light yield.

– References –

1. J. Haba, Nucl. Instr. Meth., A595 (2008) 154 – 160; **2.** N. Pavlov et al., *Nuclear Science Symposium Conference Record, 2005 IEEE* , vol.1, no., pp.173-180, 23-29 Oct. 2005; **3.** F. Corsi at al., Nuclear Science Symposium Conference Record, 2006. IEEE , vol. 2, 2006; **4.** F. Corsi et al., NIM**A** 572 (2007) 416-418; **5.** C. L. Kim, International Workshop on New Photon Detectors (PD09), PoS (PD09)010; **6.** K. Yamamoto, NIMA (2010), doi:10.1016/j.nima.2010.04.112; **7.** Hamamatsu Photonics K. K., *MPPC Technical Information*, Application Notes.

– Acknowledgments –

The authors are very thankful to the SiPM — ToF-PET group in Rutherford Appleton Laboratory, Dr. Barbara Camanzi, Dr. Mahfuza Ahmed and Dr. John Matheson for having provided some pieces of electronics and for very useful discussions. The authors want to thanks as well Dr. Fabrizio Salvatore and Mr. Edward Leming for useful discussions and suggestions.